RAPID COMMUNICATIONS

PHYSICAL REVIEW B VOLUME 51, NUMBER 20 15 MAY 1995-II

Structural characterization of (In,Ga)As quantum dots in a GaAs matrix

S. Ruvimov, P. Werner, K. Scheerschmidt, U. Gösele, and J. Heydenreich
Max-Planck-Institut für Mikrostrukturphysik, Weinberg 2, 06120 Halle/Saale, Germany

U. Richter
Labor für Elektronenmikroskopie in Naturwissenschaft und Medizin, Weinbergweg 23, 06120, Halle/Saale, Germany

N. N. Ledentsov, M. Grundmann, and D. Bimberg
Institut für Festkörperphysik, Technische Universität Berlin, Hardenbergstrasse 36, 10623 Berlin, Germany

V. M. Ustinov, A. Yu. Egorov, P. S. Kop'ev, and Zh. I. Alferov
A. F. Ioffe Physical-Technical Institute, Politekhniczeskaya 26, 194021, St. Petersburg, Russia
(Received 6 September 1994; revised manuscript received 27 December 1994)

Morphology evolution of molecular-beam-epitaxy-grown InAs and $In_{0.5}Ga_{0.5}As$ layers as a function of deposition thickness, range from 1 to 10 ML, is studied by transmission-electron microscopy to characterize the formation and the self-organization of pseudomorphic quantum dots. For deposition (at 450–480 °C) of 3–7 ML of InAs and 5–10 ML of $In_xGa_{1-x}As$, respectively, well-developed and crystallographically perfect dots with typical base length of 12 nm and small size dispersion form, which exhibit short-range ordering on a primitive two-dimensional square lattice along ⟨100⟩. The luminescence from all samples with coherent dots exhibits high quantum efficiency. For 4-ML InAs dots, coincidence of luminescence and absorption is demonstrated. Arrangement of $In_xGa_{1-x}As$ dots in chains along [110] is the result of ordering during deposition at even lower temperatures (~320 °C).

At present, there is great interest in self-organization phenomena[1–8] on crystal surfaces. The investigation of the growth of InAs and $In_xGa_{1-x}As$ quantum dots (QD's) on GaAs (Refs. 3–8) is motivated by the desire to understand the fundamental processes of nucleation and growth of thin pseudomorphic layers on their templates.[9] Furthermore, QD's are expected to exhibit unique properties like δ-function density of states leading to novel and/or strongly improved properties of photonic and electronic devices, like lasers.[10] Recently, this δ-function density of states[7,8,11] and QD lasers[12] with unique properties were demonstrated.

It was shown[3–9] that *in situ* epitaxial growth of coherently strained nanoscale islands allows attainment of a high level of quantum confinement without any patterning process. The generation of such three-dimensional (3D) islands is considered to result from a morphology evolution of the 2D layer after the growth of 1–2 ML, explained by a Stranski-Krastanov model[13] with coherent island growth. Either elastic relaxation of the strain in heterostructures, i.e., a local minimum in total energy,[14] or the kinetics of strain-induced surface roughness[15–17] have been assumed to be responsible for self-organized formation of nm-size 3D islands. However, a conclusive picture for the 2D-3D morphology transformation has not yet been established. The results of the present work demonstrate the importance of both strain and temperature, which means energetic and kinetic effects.

Our experimental results on dot size and shape differ from those reported in other work on InAs-GaAs (Ref. 3) and $In_xGa_{1-x}As$-GaAs dots,[4,5,9] grown under similar conditions. Here pyramidal-shaped dots, as known for Ge on Si,[9] are reported for InAs and $In_{0.5}Ga_{0.5}As$. Additionally self-organized short-range ordering of dots into rows along ⟨100⟩, forming a primitive two-dimensional cubic lattice, is found.

Samples were grown by molecular-beam epitaxy (MBE) using an EP1201 system. After oxide desorption, a 0.5-μm-thick GaAs buffer layer was grown at 600 °C, before the substrate temperature was reduced to a lower value T_d in order to deposit the desired amount of InAs or $In_{0.5}Ga_{0.5}As$. The nominal thickness of the deposits ranged from 1 to 10 ML. $In_{0.5}Ga_{0.5}As$ was deposited in a submonolayer growth mode[18] using 0.1-nm InAs/0.1-nm GaAs growth cycles. The growth rates were about 0.22 nm/s for GaAs and 0.08 nm/s for InAs. The arsenic pressure was kept in the range of $(2–3)\times10^{-6}$ Torr. After the deposition of the In-containing layer, two GaAs cap layers of 5 and 40 nm in thickness were subsequently grown at T_d and 600 °C, respectively. In a number of samples, two cladding superlattices of (2-nm $Al_{0.3}Ga_{0.7}As$/2-nm, GaAs)$_5$ were grown on both sides of the In-containing layer which, in this case, is inserted into a 14-nm-thick GaAs quantum well.

The evolution of InAs and $In_xGa_{1-x}As$ dots grown by MBE on GaAs (001) is studied *in situ* with reflection high-energy electron diffraction (RHEED) and *ex situ* (after the deposition of a cap layer) applying transmission electron microscopy (TEM). TEM is performed using JEOL JEM1000 (1 MV) and JEM4000EX (400 kV) microscopes. Both plan view and cross-sectional specimens are prepared for TEM studies. Low temperature ($T=8$ K) photoluminescence (PL) is used to characterize optical properties of the dots.

The *in situ* RHEED experiments show that the critical thickness for the formation of 3D islands (quantum dots) depends on layer composition, i.e., elastic energy. The criti-

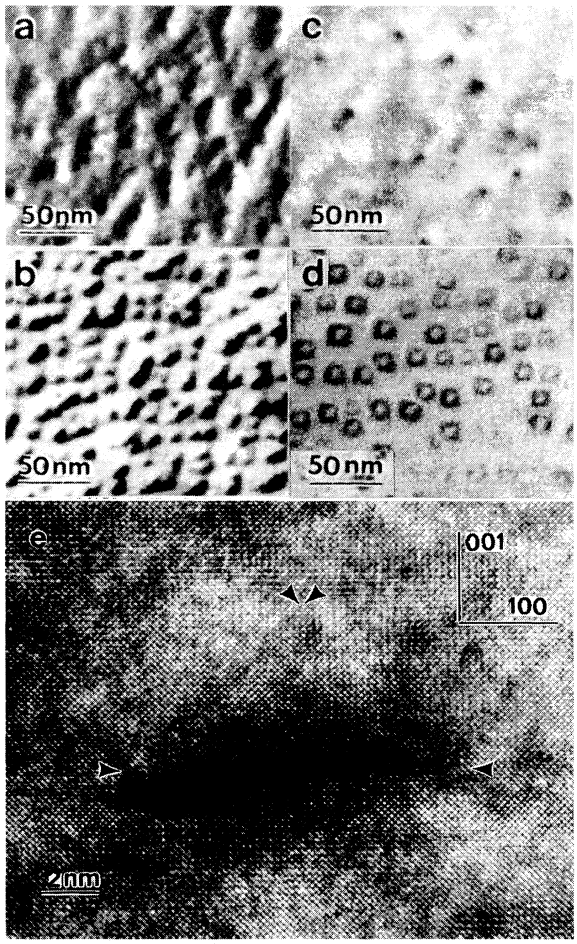

FIG. 1. Plan-view bright-field electron micrographs of (In,Ga)As quantum dots corresponding to different nominal thicknesses of In-containing layers: 3.3 ML (a) and 7.3 ML (b) of $In_{0.5}Ga_{0.5}As$, and 2 ML (c) and 4 ML (d) of InAs. Images (a)–(c) are taken at $\mathbf{g}=220$. (e) is a cross-section high-resolution electron micrograph image of a single quantum dot for 3-ML InAs deposited; arrows indicate the boundary facets.

cal thickness of $In_xGa_{1-x}As$ increases from 1.7 to 3 ML, with decreasing In content x from 1.0 to 0.5. TEM studies generally confirm this observation. Figures 1(a)–1(d) show typical plan view TEM images of In-containing layers differing in thickness (which is above the critical value in all four cases) and composition grown at $T_d=480$ °C. At the initial stages of (In,Ga)As dot formation, when slashes in the RHEED pattern just appear, the corresponding TEM images [see, e.g., Fig. 1(a) for 3.3 ML of $In_{0.5}Ga_{0.5}As$] demonstrate a fine-scale, black-and-white granular contrast composed of round-shaped dots having a diameter of approximately 60 Å. The dots appear locally connected in agglomerations. Deposition of further material leads to the formation of well-developed coherent islands and increasing size uniformity, most probably owing to the higher growth rate of relatively small islands [see Figs. 1(b) and 1(d)]. At that stage diffraction spots appears in the RHEED pattern. At a coverage of 5.3 ML of $In_{0.5}Ga_{0.5}As$, coherent islands of about 5–15 nm in size are observed. Further increase of the nominal thickness of $In_{0.5}Ga_{0.5}As$ up to 7.3 ML results in the formation of well-developed dots with reduced variation of size and spacing [Fig. 1(b)].

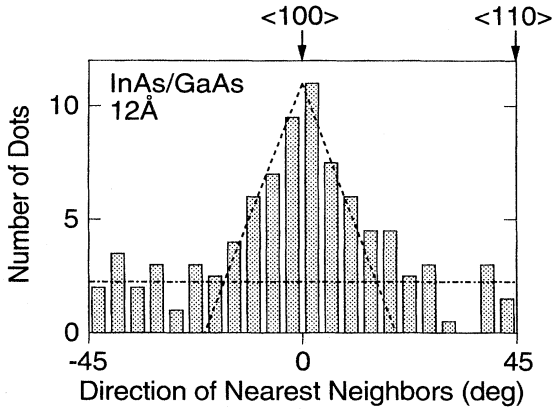

FIG. 2. Histogram of next-neighbor dot direction (moduls 90°) for 4-ML InAs, obtained from a TEM image like Fig. 1(d). Dashed line is expected for partially disordered square lattice, dash-dotted line for superposed random dot distribution.

The formation of well-developed InAs dots (at $T_d=480$ °C) begins already at an average thickness of less than 2 ML. Figures 1(c) and 1(d) show dots formed during InAs deposition of nominal thicknesses of 2 and 4 ML, respectively. A comparison of the results for deposition of InAs and $In_{0.5}Ga_{0.5}As$ indicates that the onset of dot formation is governed by the strain energy per interface area.

There is a distinct difference in dot density and contrast for the different layers shown in Fig. 1. The $In_{0.5}Ga_{0.5}As$ dots in Fig. 1(b) are closely packed and ordered approximately parallel to the ⟨100⟩ directions. They have a black-and-white contrast probably resulting from the strain introduced by the high lattice mismatch between the dots and the GaAs matrix. The black-white transition is perpendicular to the diffraction vectors $\mathbf{g}$ of (220) or (400) type indicating a symmetrical strain distribution with {100} and {110} symmetry planes. Such a contrast is typical for regular arrangement of small precipitates as well as for a dislocation network. The dots in Fig. 1(b) have pyramidal shape with base sides parallel to ⟨100⟩. The beginning of dislocation nucleation is also observed in this sample, probably a consequence of local inhomogeneities of the In distribution.

Figure 1(d) and 1(e) indicate that InAs dots also are of pyramidal shape with a square base. This is already known for Ge clusters on Si(001).[9] The pyramid's principal axes are close to the two orthogonal ⟨100⟩ directions. The average length of the dot base is about 12 ± 1 nm. The dot geometry is additionally evidenced by the cross-section image in Fig. 1(e). The height of the dots is found to be about 6 nm. The sidewalls are close to {110}. Also the InAs dots align in rows along ⟨100⟩ and demonstrate the symmetry of a two-dimensional primitive square lattice as can be seen from Fig. 1(d). A histogram of the direction of next-neighbor dots (Fig. 2) has been obtained from a statistical analysis of a TEM image. It clearly has a maximum at the ⟨100⟩ direction confirming the subjective impression from the image Fig. 1(d). The dashed line in Fig. 2 is the expected dependence for dots

on a partially disordered square lattice. The self-ordering is superposed by some randomness, resulting in an offset (dash-dotted line) independent of the azimuth.

A quantitative comparison of the dot sizes for different samples is rather difficult due to the influence of dot size of the diffraction contrast. For example, the average size of the dots for 2-ML InAs [Fig. 1(c)] is similar to that of 3.3-ML $In_{0.5}Ga_{0.5}As$ and smaller than that of 4-ML InAs. Resulting decrease of dot-induced deformation leads to a relatively weak contrast in Fig. 1(c) where the dots also do not show a clearly distinguishable crystallographic shape. For 4-ML InAs we measured the dot size more precisely under diffraction conditions far away from the exact Bragg orientation, so that the strong strain contrast is remarkably reduced [Fig. 1(d)]. The size distribution of the dots of 2- and 4-ML InAs samples is rather narrow ($<20\%$) and similar to results reported in Ref. 5. The variation of dot size and interdot distance at the initial stages of dot deformation for $In_{0.5}Ga_{0.5}As$ deposition is found to be larger than that for the InAs deposition.

For deposition conditions similar to those in Ref. 5 we have found InAs dots of approximately the same size. However, the size of the dots formed after 2.3-ML InAs deposition at 500 °C reported in Ref. 3 is twice as large as ours. Thus either AFM yields an overestimate of the size of the dots or dot formation is extremely sensitive to the growth conditions. Our results about the $In_xGa_{1-x}As$ dot sizes disagree with values reported in Ref. 4 but are corroborated by more recent results.[5]

We have observed that at advanced stages of dot formation (nominal large average layer thickness) the lateral dimensions of InAs and $In_xGa_{1-x}As$ dots are almost identical as long as the coverage is below the onset of dislocation formation. Thus, it seems that there is an energetically favorable size of the islands as, e.g., for ordered surface faceting[2,18] or for the spontaneous formation of quantum wires.[19,20] Growth kinetics is likely to strongly affect the initial stage of layer transformation at extremely low substrate temperatures. Regular distribution of the dots can be a result of two alternative processes, namely, of the ordering of nucleation centers on the surface followed by equalization of dot sizes during further material deposition and/or by strain-field-induced ordering with increasing coverage. Indeed, periodic lateral modulations of layer composition have been observed in highly strained heterostructures[21] resulting from the spinodal decomposition of ternary or quaternary solid solutions. Similar effects may also accompany the formation of the first one or two ML of $In_xGa_{1-x}As$ resulting in a quasiperiodic lateral strain/composition distribution and, hence, in a regular arrangement of the nucleation centers of 3D islands. Further development of the 3D islands is associated with the redistribution and minimization of the strain in the layer, leading to a minimization of the total energy. Thus, one can expect the existence of an equilibrium dot size[22] associated with a total-energy minimum at larger layer thickness. We suppose that the ordered array represents an energetic minimum configuration as well.

Actually, the layer morphology (distribution and shape of dots) is found to strongly depend on growth conditions, namely, the deposition temperature. Reducing the substrate temperature for $In_{0.5}Ga_{0.5}As$ growth down to 320 °C results

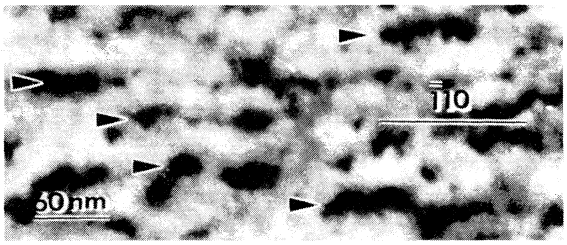

FIG. 3. Plan-view bright-field TEM image ($\mathbf{g}=220$) of 3.3-ML $In_{0.5}Ga_{0.5}As$ grown at 320 °C.

in the ordering of dot agglomerations parallel to [110] (see Fig. 3). This is, to our knowledge, the first observation of such a chainlike arrangement of quantum dots. The surface appears wavy with a characteristic spacing of 50 nm between neighboring chains. Additionally there are individual dots in between the chains. The anisotropy in the dot arrangement observed in Fig. 3 agrees fairly well with that observed for InAs submonolayer grown on GaAs,[19,20] and is believed to be connected with a particular kinetic pathway.

The optical properties of the dots are correlated with the morphology obtained from TEM. Generally the dots exhibit high internal quantum efficiency close to 100% at low temperatures. Figure 4 depicts PL spectra of the structures with 2 and 4 ML of InAs. They differ in peak position and intensity in accordance with the TEM data on size and distribution of the dots. The smaller dots with larger dispersion give rise to a weaker and broader PL line which is also closer to the GaAs band-gap energy as compared to the PL peak of the larger dots showing a more homogeneous size distribution. The small density of quantum-dot-induced states in 2-ML InAs dots is not distinguishable in the absorption spectrum, which is dominated by the large density of states in the residual untransformed 2D layer. For a dense array of uniform InAs dots [Fig. 1(d)], however, the absorption peak of the dot

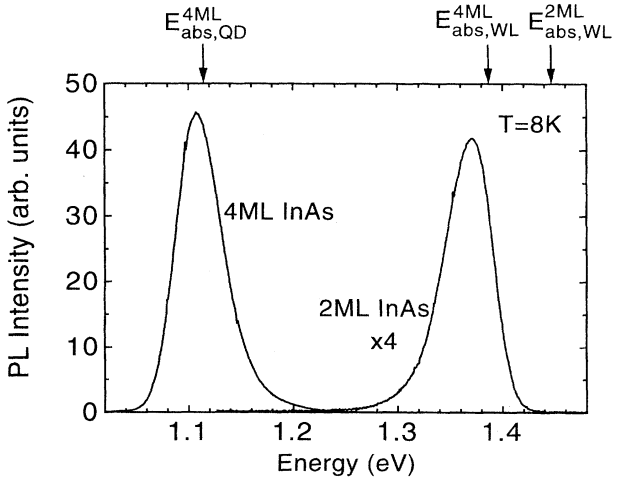

FIG. 4. Low-temperature ($T=8$ K) PL spectra of quantum dots in samples with 2 and 4 ML of InAs at excitation density $D=1$ W cm^{-2}. The peak energies in the absorption spectra for the wetting layer (WL) in both samples and the quantum dots in the 4-ML sample are shown by arrows.

ground state is clearly identified and coincides with the PL maximum (the absorption of the wetting layer being present additionally also here).

The corrugation of the $In_{0.5}Ga_{0.5}As$ layer [Fig. 1(a)] revealed by TEM at the initial stage of layer transformation has also a strong effect on luminescence properties resulting in an intense PL peak which is shifted from the position expected for a uniform $In_xGa_{1-x}As$ layer (~ 1.4 eV for a 1-nm-thick $In_{0.5}Ga_{0.5}As$ layer) (Ref. 23) to lower energies. The structures with 3.3–4 ML of $In_{0.5}Ga_{0.5}As$ deposited at 400–450 °C exhibit the PL peak at 1.23–1.26 eV with 40–60 meV as the full width at half maximum (FWHM). Here we observe a large Stokes shift between the PL line (1.24 eV) and the absorption (1.31 eV) indicating a nonuniform size distribution of $In_xGa_{1-x}As$ dots. The ordering of $In_xGa_{1-x}As$ clusters in a chainlike structure at lower deposition temperatures ($T_d = 320$ °C) (Fig. 3) results in a narrow line (FWHM is ~ 12 meV, only). The line is shifted to higher energies (1.3 eV) relative to the PL line position at higher deposition temperatures (1.24 eV at 400 °C) and almost coincides with a sharp peak observed in the absorption spectrum indicating good average uniformity of this arrangement.

In summary, the formation of ordered arrays (forming a primitive two-dimensional cubic lattice) of pseudomorphic dots of pyramidal-like shape, typically 6 nm in height and about 12 nm in base diameter, has been observed on a residual two-dimensional layer above a nominal coverage of 2 ML for InAs and 6 ML for $In_{0.5}Ga_{0.5}As$ on GaAs. The dispersion of dot size and interdot distance was found to be remarkably low (<20%). Efficient luminescence from dot states has been observed for all samples. For dense dot arrays ($\sim 10^{11}$ dots/cm^2) grown under optimum conditions, the quantum dot ground-state photoluminescence and absorption were found to coincide energetically. At low deposition temperature ($T_d = 320$ °C), $In_{0.5}Ga_{0.5}As$ layers arrange in an array of chains along [110], exhibiting high quantum efficiency as well.

This work was partly supported by the Volkswagen Stiftung, by INTAS, and by Deutsche Forschungsgemeinschaft in the framework of Sfb 296.

[1] P. M. Petroff, J. Gaines, M. Tsuchiya, R. Symes, L. Coldren, H. Kroemer, J. English, and A. C. Gossard, J. Cryst. Growth **95**, 260 (1989).

[2] R. Nötzel, N. N. Ledentzov, L. Däweritz, M. Hohenstein, and K. Ploog, Phys. Rev. Lett. **67**, 3812 (1991).

[3] J. M. Moison, F. Houzay, F. Barthe, L. Leprice, E. Andre, and O. Vatel, Appl. Phys. Lett. **64**, 196 (1994).

[4] D. Leonard, M. Krishnamurthy, C. M. Reaves, S. P. Denbaars, and P. M. Petroff, Appl. Phys. Lett. **63**, 3203 (1993).

[5] D. Leonard, M. Krishnamurthy, S. Fafard, J. L. Merz, and P. M. Petroff, J. Vac. Sci. Technol. B **12**, 1063 (1994).

[6] R. Nötzel, J. Temmyo, and T. Tamamura, Nature (London) **369**, 131 (1994).

[7] N. N. Ledentsov, M. Grundmann, N. Kirstaedter, J. Christen, R. Heitz, J. Böhrer, F. Heinrichsdorff, D. Bimberg, S. S. Ruvimov, P. Werner, U. Richter, U. Gösele, J. Heydenreich, V. M. Ustinov, P. S. Kop'ev, and Zh. I. Alferov, in *Proceedings of the 22nd International Conference on the Physics of Semiconductors, Vancouver, Canada, 1994* (World Scientific, Singapore, 1995).

[8] M. Grundmann, N. Ledentsov, J. Christen, J. Böhrer, D. Bimberg, S. Ruvimov, P. Werner, U. Richter, U. Gösele, J. Heydenreich, V. M. Ustinov, A. Yu. Egorov, A. E. Zhukov, P. S. Kop'ev, and Zh. I. Alferov, Phys. Status Solidi (to be published).

[9] Y.-W. Mo, D. E. Savage, B. S. Swartzentruber, and M. G. Lagally, Phys. Rev. Lett. **65**, 1020 (1990).

[10] Y. Arakawa and H. Sakaki, Appl. Phys. Lett. **40**, 939 (1982).

[11] J.-Y. Marzin, J.-M. Gérard, A. Izrael, D. Barrier, and G. Bastard, Phys. Rev. Lett. **73**, 716 (1994).

[12] N. Kirstaedter, N. N. Ledentsov, M. Grundmann, D. Bimberg, V. M. Ustinov, S. S. Ruvimov, M. V. Maximov, P. S. Kop'ev, Zh. I. Alferov, U. Richter, P. Werner, U. Gösele, and J. Heydenreich, Electron. Lett. **30**, 1416 (1994).

[13] I. N. Stranski and L. Krastanow, Sitzungsber. Akad. Wiss. Wien Math. Naturwiss. Kl. Abt. 2B Chemie **146**, 797 (1937).

[14] D. J. Eaglesham and M. Cerullo, Phys. Rev. Lett. **64**, 1943 (1990).

[15] A. Madhukar, Q. Xie, P. Chen, and A. Konkar, Appl. Phys. Lett. **64**, 2727 (1994).

[16] C. W. Snyder, B. G. Orr, D. Kessler, and L. M. Sander, Phys. Rev. Lett. **66**, 3032 (1991).

[17] B. G. Orr, D. Kessler, C. W. Snyder, and L. Sander, Europhys. Lett. **19**, 33 (1992).

[18] V. I. Marchenko, Zh. Eksp. Teor. Fiz. **81**, 1141 (1981) [Sov. Phys. JETP **54**, 605 (19981)].

[19] P. D. Wang, N. N. Ledentsov, C. M. Sotomayor Torres, P. S. Kop'ev, and V. M. Ustinov, Appl. Phys. Lett. **64**, 1526 (1994).

[20] V. Bressler-Hill, A. Lorke, S. Varma, P. M. Petroff, K. Pond, and W. H. Weinberg, Phys. Rev. B **50**, 8479 (1994).

[21] F. Glas, C. Gors, and P. Henoc, Philos. Mag. B **62**, 373 (1990).

[22] J. Tersoff and R. M. Tromp, Phys. Rev. Lett. **70**, 2782 (1993).

[23] A. Ksendzov, F. J. Grunthaner, J. L. Liu, D. H. Rich, R. W. Terhune, and B. A. Wilson, Phys. Rev. B **43**, 1475 (1991).

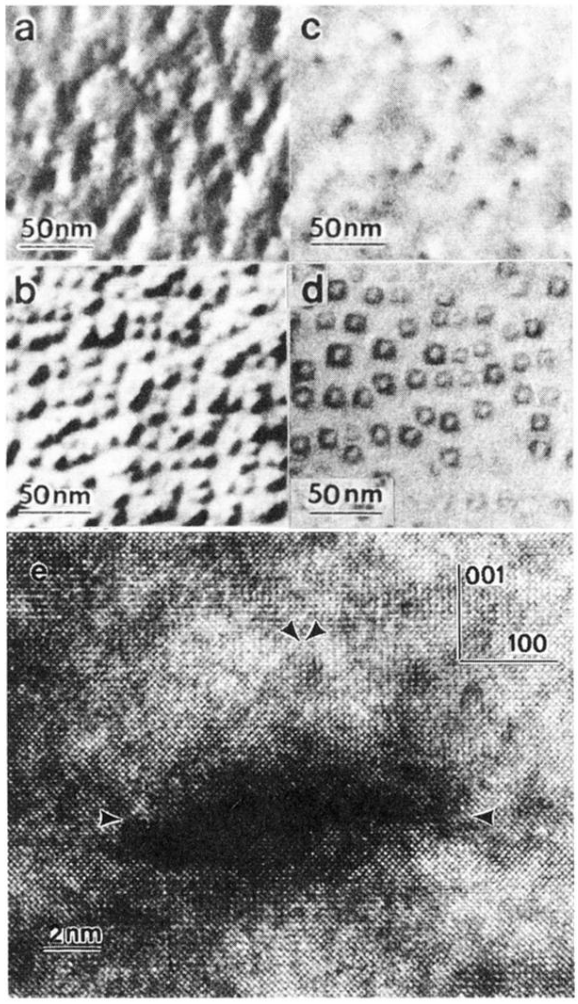

FIG. 1. Plan-view bright-field electron micrographs of (In,Ga)As quantum dots corresponding to different nominal thicknesses of In-containing layers: 3.3 ML (a) and 7.3 ML (b) of $In_{0.5}Ga_{0.5}As$, and 2 ML (c) and 4 ML (d) of InAs. Images (a)–(c) are taken at $\mathbf{g}=220$. (e) is a cross-section high-resolution electron micrograph image of a single quantum dot for 3-ML InAs deposited; arrows indicate the boundary facets.

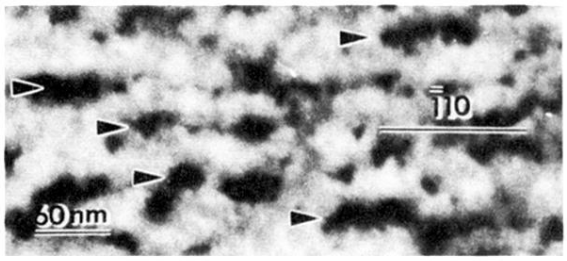

FIG. 3. Plan-view bright-field TEM image ($\mathbf{g}=220$) of 3.3-ML $In_{0.5}Ga_{0.5}As$ grown at 320 °C.